Variational denoising method for electronic speckle pattern interferometry

Fang Zhang (张 芳)[1,2], Wenyao Liu (刘文耀)[1,2], Chen Tang (唐 晨)[3], Jinjiang Wang (王晋疆)[1,2], and Li Ren (任 丽)[1,2]

[1] *College of Precise Instrument and Optical Electronic Engineering, Tianjin University, Tianjin 300072*

[2] *Key Laboratory of Opto-Electronics Information Technical Science, Ministry of Education, Tianjin 300072*

[3] *Department of Applied Physics, Tianjin University, Tianjin 300072*

Received July 16, 2007

Traditional speckle fringe patterns by electronic speckle pattern interferometry (ESPI) are inherently noisy and of limited visibility, so denoising is the key problem in ESPI. We present the variational denoising method for ESPI. This method transforms the image denosing to minimizing an appropriate penalized energy function and solving a partial differential equation. We test the proposed method on computer-simulated and experimental speckle correlation fringes, respectively. The results show that this technique is capable of significantly improving the quality of fringe patterns. It works well as a pre-processing for the fringe patterns by ESPI.

OCIS codes: 110.6150, 030.6140, 100.0100.

Electronic speckle pattern interferometry (ESPI) is a well-known nondestructive and whole-field technique for applications such as vibration measurement, measurement of displacements and their derivatives[1−6]. However, the digital speckle fringe patterns of ESPI are inherently full of speckle noise and of limited visibility, which causes difficulties in post-processing of phase extraction. Therefore research on effective denoising in fringe patterns by ESPI is a key problem for application of ESPI technique. Unfortunately, the traditional spatial filtering and frequency filtering methods usually result in blurring effect. The filtering method based on partial differential equations (PDEs) has become an interest-raising research topic in the past few years[7−10], the main idea of which is transforming the image processing to solving PDEs. This method has been successfully applied in ESPI and its validity has been illustrated[11]. Image denoising can also be obtained by variational method[9,12,13] and this method seems to work well for images represented by functions of bounded variation which includes step functions[9]. The main idea of this method is enhancing a noised image by minimizing an appropriate penalized energy function. Using Euler-Lagrange equation, a PDE can be obtained from the energy function. Then the filtered image can be reconstructed by solving this equation.

We apply the variational method in the fringe patterns by ESPI in this paper, and test the proposed method on the computer-simulated and experimental speckle correlation fringes, respectively. The results show that the technique can significantly improve the quality of correlation speckle fringe patterns. It works well as a pre-processing for the fringe patterns by ESPI.

For a noised image I defined on an image domain Ω, let u be a denoised image defined as a minimizer for the function[13]

$$E(u) = \int_{\Omega} \phi\left(|\nabla u|\right) \mathrm{d}x\mathrm{d}y + \frac{\lambda}{2} \int_{\Omega} |u - I|^2 \, \mathrm{d}x\mathrm{d}y, \qquad (1)$$

for which the necessary optimality condition is expressed in the steady state for the following descent minimization method:

$$\partial_t u = \nabla \cdot \left(c(|\nabla u|)\nabla u\right) - \lambda\left(u - I\right),$$

$$u(0) = I, \quad \Omega \times [0, \infty). \qquad (2)$$

In Eq. (2), $\nabla\cdot(c(|\nabla u|)\nabla u)$ is the diffusion term, and here, the variational penalty function ϕ gives the diffusivity $c(s) = \phi'(s)/s$; $\lambda\left(u - I\right)$ is the fidelity term and λ is the fidelity coefficient. The two terms work together to smooth the initial noisy image.

Although there are many other variational methods, we will only mention Perona-Malik (PM) model here, which is now one of the most successful tools for image restoration. Considering the following form of ϕ,

$$\phi_{\mathrm{PM}}\left(|\nabla u|\right) = \frac{1}{2k} \ln\left(1 + k\left|\nabla u\right|^2\right), \qquad (3)$$

where k is a constant parameter and the restoration u can be obtained by minimizing the energy function

$$E_{\mathrm{PM}}(u) = \frac{1}{2k} \int_{\Omega} \ln\left(1 + k\left|\nabla u\right|^2\right) \mathrm{d}x\mathrm{d}y$$

$$+ \frac{\lambda}{2} \int_{\Omega} |u - I|^2 \, \mathrm{d}x\mathrm{d}y. \qquad (4)$$

The Euler-Lagrange optimality equation for this problem is now

$$\nabla \cdot \left(\frac{1}{1 + k\left|\nabla u\right|^2} \nabla u\right) - \lambda\left(u - I\right) = 0,$$

$$u(0) = I, \quad \Omega \times [0, \infty). \qquad (5)$$

Let[9]

$$c_k\left(s\right) = \left(1 + ks^2\right)^{-1}, \qquad (6)$$

1671-7694/2008/010038-03

consequently, we expect that the evolution equation

$$\partial_t u = \nabla \cdot (c(|\nabla u|)\nabla u) - \lambda (u - I). \tag{7}$$

If $\lambda = 0$, Eq. (7) shows the famous PM anisotropic diffusion equation[7]. In model (7), the diffusivity $c(|\nabla u|)$ is used for controlling the speed of diffusion: if ∇u has a small value in a neighborhood of a point (x, y), this point (x, y) is considered as an interior point of a smooth region of the image and the diffusion is therefore strong; if ∇u has a large value in the neighborhood of (x, y), (x, y) is considered as an edge point and the diffusion speed is lowered, since $c(s)$ is small for large s. Therefore the method has good edge protection capability. However, this model still has a shortcoming. The noise introduces very large oscillations of the gradient ∇u. Thus the value of $c(|\nabla u|)$ is very small and the noise edges will be kept using the model (7).

Here, we adopt a modification of the PM model developed by Catté *et al.*[8] for ESPI. This model replaces $c(|\nabla u|)$ in PM model by $c(|\nabla G_\sigma * u|)$, where G_σ is a Gaussian smoothing kernel[8],

$$G_\sigma (x, y) = C\sigma^{-1/2} \exp\left(-(x^2 + y^2)/4\sigma\right). \tag{8}$$

Correspondingly, the filtering PDE can be shown as

$$\partial_t u = \nabla \cdot (c(|\nabla G_\sigma * u|)\nabla u) - \lambda (u - I),$$

$$u(0) = I, \quad \Omega \times [0, \infty). \tag{9}$$

In model (9), $\nabla G_\sigma * u$ appears to be an estimate of the gradient of u at point (x, y). Indeed, the equation will diffuse only if the gradient is estimated to be small. Therefore, the isolated noise, which has the large value of ∇u but small value of $\nabla G_\sigma * u$, will be eliminated through the high diffusion speed, whereas, the true edge, which has the large value of $\nabla G_\sigma * u$, will be preserved. To sum up, Eq. (9) has two advantages. The diffusivity $c(|\nabla G_\sigma * u|)$ is small when $\nabla G_\sigma * u$ is big, so that minimal smoothing is acquired around the edge of the image. Furthermore, Gaussian smoothing avoids noise sensitivity.

For computing Eq. (9) numerically, we attempt to discretize it. Our images are represented by $M \times N$ matrices of intensity values. So, for any function (i.e., image) $u(x, y)$, we let $u_{i,j}$ denote $u(i, j)$ for $1 \le i \le M$, $1 \le j \le N$. The evolution equation obtains images at times $t_n = n\Delta t$. We denote $u(i, j, t_n)$ by $u^n_{i,j}$.

The time derivative u_t at (i, j, t_n) is approximated by the forward difference

$$(u_t)^n_{i,j} = \frac{u^{n+1}_{i,j} - u^n_{i,j}}{\Delta t}, \tag{10}$$

where Δt is time step size.

The spatial derivatives are

$$(u_x)^n_{i,j} = \frac{u^n_{i+1,j} - u^n_{i-1,j}}{2}, \ (u_y)^n_{i,j} = \frac{u^n_{i,j+1} - u^n_{i,j-1}}{2}. \tag{11}$$

And the boundary conditions are

$$u^n_{i,0} = u^n_{i,1}, \ u^n_{i,N+1} = u^n_{i,N}, \ i = 1, 2, \cdots, M, \tag{12a}$$

$$u^n_{0,j} = u^n_{1,j}, \ u^n_{M+1,j} = u^n_{M,j}, \ j = 1, 2, \cdots, N. \tag{12b}$$

We denote $\beta^n_{i,j}$ as an approximation of $c(|\nabla G_\sigma * u(i, j, t_n)|) = (1 + k(|\nabla G_\sigma * u(i, j, t_n)|)^2)^{-1}$. Then we discretize $\nabla \cdot (c(|\nabla G_\sigma * u|)\nabla u)$ in Eq. (9) by

$$\varphi^n_{i,j} = \frac{(\beta u_x)^n_{i+1,j} - (\beta u_x)^n_{i-1,j}}{2} + \frac{(\beta u_y)^n_{i,j+1} - (\beta u_y)^n_{i,j-1}}{2}. \tag{13}$$

Finally, we obtain the explicit discrete scheme of Eq. (9) as

$$u^{n+1}_{i,j} = u^n_{i,j} + \Delta t \left(\varphi^n_{i,j} - \lambda(u^n_{i,j} - I_{i,j})\right). \tag{14}$$

For evaluating the real performance of PDE enhancement-denoising method, we tested the proposed method on the computer-simulated speckle correlation fringe and experimentally obtained fringe, respectively, and compared it with traditional mean filtering and low-pass Fourier filtering.

Figure 1(a) gives a computer-simulated original fringe pattern. The computer-simulated fringe was generated by means of the method reported in Ref. [4] based on

$$I_{\text{sub}} = \left|4\sqrt{I_{\text{o}} I_{\text{r}}} \sin\left(\phi_{\text{r}} - \phi_{\text{o}} + \frac{\varphi}{2}\right) \sin\left(\frac{\varphi}{2}\right)\right|, \tag{15}$$

where I_{o} and I_{r} are the intensities of the object and the reference beams, respectively; $(\phi_{\text{r}} - \phi_{\text{o}})$ is the random interferometric phase of the speckle field and φ is the phase change due to the deformation of surface of the tested object. The fringe pattern by ESPI can be simulated with $\phi_{\text{r}} - \phi_{\text{o}}$, I_{o} and I_{r} taken as random variables with values uniformly distributed over the intervals $[-\pi, \pi]$, $[0, I_m]$, and $[0, \rho I_m]$, respectively, where I_m is a constant value and ρ is a normalized visibility parameter. Figure 1(a) shows a simulated speckle pattern with $I_m = 250$,

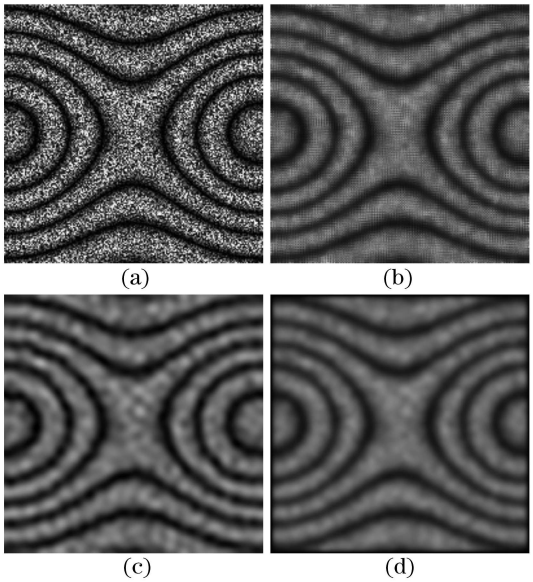

Fig. 1. Computer-simulated fringe pattern by ESPI and its filtered images. (a) Original fringe pattern; (b) variational denoised image by model (9); (c) low-pass Fourier filtered image; (d) mean filtered image.

$\rho = 0.2$, and $\varphi(x, y)$ calculated from

$$\varphi(x,y) = 40\left[\exp\left(-\frac{(x-0.5M)^2+y^2}{8000}\right) + \exp\left(-\frac{(x-0.5M)^2+(y-N)^2}{8000}\right)\right]. \quad (16)$$

Figure 1(b) shows the filtered image by performing model (9) with $\Delta t = 0.5$, $n = 10$, $k = 0.001$ and $\lambda = 0.1$. Figure 1(c) gives its low-pass Fourier filtered image with frequency threshold value $D_0 = 20$. Figure 1(d) is the mean filtered image for 10 iterations.

In further studies, an experimental fringe pattern was tested. The original fringe is shown in Fig. 2(a), it is a digital speckle shearing interferometry (DSSI) fringe pattern[2]. Figure 2(b) shows the filtered image by performing model (9) with $\Delta t = 0.25$, $n = 10$, $k = 0.001$ and $\lambda = 0.1$. Figure 2(c) gives its low-pass Fourier filtered image with frequency threshold value $D_0 = 25$. Figure 2(d) is the mean filtered image for 10 iterations.

As we can see from the original images, the noises in the fringe patterns are high. It is apparent that the proposed variational denoising method performs significantly well in filtering and preserving the edges of the fringes, which can be seen in Figs. 1(b) and 2(b). While the edge of the fringes are destroyed heavily by performing low-pass Fourier filter and mean filter methods, which can be seen in Figs. 2(c) and (d). The experimental results show that the PDE filtered fringe patterns can provide better visual inspections as compared with these well-known traditional techniques. It works well as a pre-processing for the fringe patterns by ESPI.

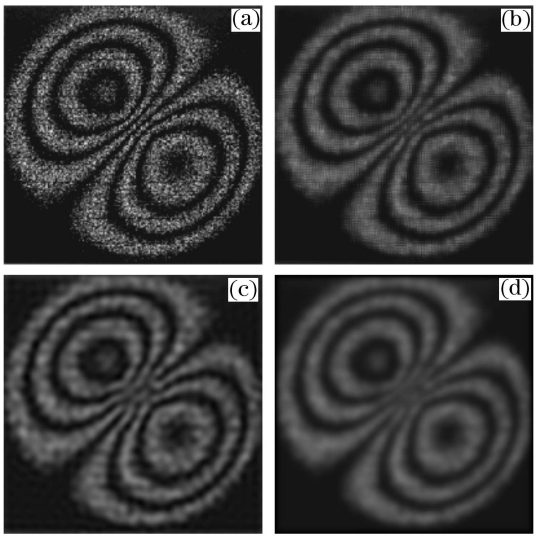

Fig. 2. Experimental fringe pattern and its filtered images. (a) Original fringe pattern; (b) variational denoised image by model (9); (c) low-pass Fourier filtered image; (d) mean filtered image.

In conclusion, we apply the variational denoising method to the ESPI. The denoised image is reconstructed as the solution of an equation, which is obtained by minimizing an appropriate penalized energy function. The energy function contains both the diffusion term and the fidelity term, which work together to smooth the initial noisy image. The main advantage of the method is that it has both good noise reduction and edge protection capabilities. Therefore it improves the quality of ESPI fringes significantly.

F. Zhang's e-mail address is hhzhangfang@126.com.

References

1. M. J. Huang, Z.-N. He, and F.-Z. Lee, Measurement **36,** 93 (2004).
2. C. Quan, C. J. Tay, F. Yang, and X. He, Appl. Opt. **44,** 4814 (2005).
3. R. Ambu, F. Aymerich, F. Ginesu, and P. Priolo, Compos. Sci. Technol. **66,** 199 (2006).
4. N. A. Ochoa, F. M. Santoyo, A. J. Moore, and C. P. López, Appl. Opt. **36,** 2783 (1997).
5. K. H. Womack, Opt. Eng. **23,** 391 (1984).
6. P. Sun, L. Zhang, and C. Tao, Acta Photon. Sin. (in Chinese) **34,** 1074 (2005).
7. P. Perona and J. Malik, IEEE Trans. Pattern Analysis and Machine Intelligence **12,** 629 (1990).
8. F. Catté, P.-L. Lions, J.-M. Morel, and T. Coll, SIAM J. Numer. Anal. **29,** 182 (1992).
9. Y. Chen, C. A. Z. Barcelos, and B. A. Mair, Comput. Vis. Image Understand. **82,** 85 (2001).
10. W. Qian, R. Liu, W. Wang, S. Qi, W. Wang, and J. Cheng, Journal of Image and Graphics (in Chinese) **11,** 818 (2006).
11. C. Tang, F. Zhang, H. Yan, and Z. Chen, Opt. Commun. **260,** 91 (2006).
12. L. I. Rudin, S. Osher, and E. Fatemi, Phys. D **60,** 259 (1992).
13. S. L. Keeling, Appl. Math. Comput. **139,** 101 (2003).